Proceedings of the 5th WSEAS Int. Conf. on SIMULATION, MODELING AND OPTIMIZATION, Corfu, Greece, August 17-19, 2005 (pp365-372)

Quench Process Optimization for Receiving Super Strong Materials

NIKOLAI KOBASKO

Intensive Technology Ltd., Kyiv, Ukraine
IQ Technologies Inc., Akron, USA

Abstract:- The paper presents an analytical dependence for the determination of ideal critical diameter of DI, and also equations for interruption of intensive quenching to provide optimal quenched layer. On the basis of the results obtained, steels of low, usual and high hardenability can be used to provide optimal stress distribution and receive super strong materials. It discusses also the conditions of intensive quenching and similarity in the distribution of residual stresses in parts quenched, which allow to extend the results of studies obtained with small parts to large-scale parts. It has been shown that the low-hardenability steels provide the optimal depth of hardened layer for small parts, for example, teeth of gears and rolling bearings, and so on, which increase their service life by several times. It is for the first time that a simple method of calculating the optimal depth of hardened layer for small and large parts has been suggested. This approach significantly simplifies the calculations and allows to optimize the processes of quench cooling for both large and small parts. The equations obttained are the basis for designing simplified software to govern the quenching processes.

Keywords:- Hardenability, Critical size, Optimal quenched layer, Optimal stress distribution, Compressive stresses, Service life, Super strong materials.

1 Analitical Calculation of Critical Diameter DI

The generalized dependence for the calculation of cooling time for bodies of arbitrary geometries, obtained in the analytical form in Ref.(1), may be easily transformed for the calculation of an ideal critical diameter. Actually, the generalized dependence can be presented as follows:

$$D = \left(\frac{\underline{a} b \underline{Kn} \tau_m}{\Omega + \ln \theta} \right)^{0.5}, \qquad (1)$$

where D is the characteristic size (diameter of cylinder, ball, thickness of plate, and so on (m)),

$\underline{a}$ is average thermal diffusivity (m^2/s);

$\underline{Kn}$ is Kondratjev number (dimensionless value);

τ_m is limit time of the core cooling from the austenitizing temperature to martensite start temperature, providing the creation of 99% or 50% martensite (see Fig. 1);

$\Omega = 0.48$ for a bar (or cylinder);

$$\theta = \frac{T_0 - T_m}{T_M - T_m};$$

T_0 is austenitizing temperature;

T_m is temperature of quenchant;

T_M is martensite start temperature at limit time of cooling (see Fig. 1).

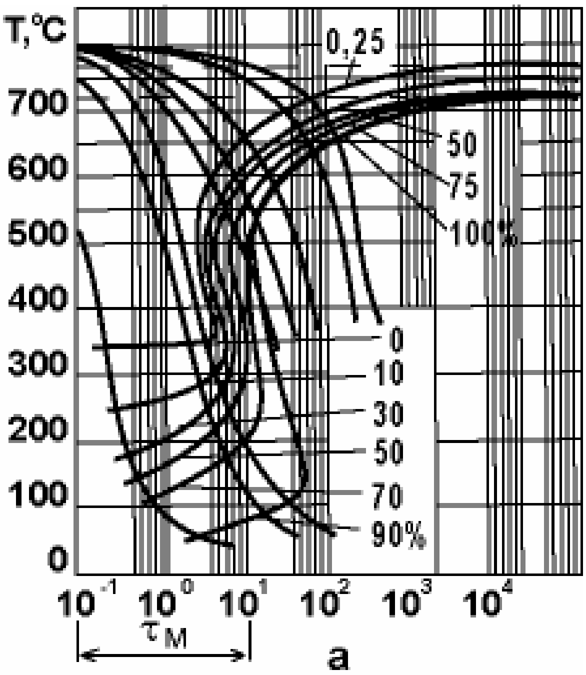

Fig. 1 CCT diagrams for AISI 1045 steel

As known, the ideal cooling conditions assume $Bi \to \infty$, and this means that under these conditions $\overline{Kn}$ is equal to 1. Therefore, formula (1) is reduced as follows:

$$DI = \left(\frac{\bar{a} b \tau_M}{\Omega + \ln\theta} \right)^{0.5} \qquad (2)$$

The advantage of equation (2) is that it allows to calculate critical diameters for bodies of any geometry at any required percentage of the martensite in the core. Here there must be available CCT diagrams presenting the information about the quantity of martensite formed in the body.

Parameter *b* depends on the shape of the body, and it is obtained by transforming from Kondratjev form coefficient K to a specific value of a diameter or thickness of the part.

For example, Kondratjev form coefficient is $K = \frac{L^2}{9.87}$ for unbounded plate; $K = \frac{D^2}{23.13}$ for infinit

cylinder; $K = \frac{D^2}{39.48}$ for a ball.

Therefore, value of *b* for a plate, cylinder and ball is 9.87, 23.13 and 39.48 relatively.

It is of interest to determine the precision of calculations. For the comparison of calculated data, Table 1 presents results of calculations compared with results published in Ref.(2). It is obvious from Table 1 that the results of calculations agree well with results [2]. Of course, the results of calculations depend on the accuracy of CCT diagram and thermophysical properties of material, in particular, thermal diffusivity $\bar{a}$.

Table 1 Chemical composition and hardenability

Steel Grade	C	Si	Mn	P	S	Cu	Cr	Ni	Mo	B	DI, mm	DI$_{\text{calculation}}$ mm
C45	0.46	0.25	0.72	0.016	0.033	0.22	0.12	0.13	0.01		31.5(29)	30.10
C55	0.55	0.29	0.77	0.022	0.022	0.18	0.13	0.07	0.01		37 (33)	38.80
25CrMo4	0.25	0.24	0.61	0.015	0.028	0.19	1.02	0.12	0.17		76.2 (75)	
30MnB CrB	0.32	0.25	1.23	0.015	0.011	0.26	0.52	0.11	0.02	0.003	122.4 (119)	
* Boronfactor 1.77												

2 Criterion Determining the Absence of Self-Regulated Thermal Process

We can draw the criterion determining the absence of nucleate boiling at the surface of a part to be quenched on the basis of the generalized dependence for the determination of the duration of non-stationary nucleate boiling, i.e., self-regulated thermal process. As is already known, the specified dependence has the following form

$$\tau = \left[\Omega + b \ln \frac{\vartheta_I}{\vartheta_{II}} \right] \frac{K}{a} \qquad (3)$$

In this formula the value of Ω determines the duration of irregular thermal process and is quite a small value. The duration of the established non-stationary nucleate boiling is determined basically by the second term of dependence (2), i.e $b \ln \frac{\vartheta_I}{\vartheta_{II}}$. To avoid nucleate boiling, it is necessary that the second part of formula (3) is equal to zero, i.e., $b \ln \frac{\vartheta_I}{\vartheta_{II}} = 0$.

We have obtained equations for ϑ_I and ϑ_{II}, which can be presented as:

$$\vartheta_I = \frac{1}{\beta} \left[\frac{2\lambda(\vartheta_0 - \vartheta_I)}{R} \right]^{0.3} \qquad (4)$$

and

$$\vartheta_{II} = \frac{1}{\beta} \left[\alpha_{conv} (\vartheta_{II} + \vartheta_{uh}) \right]^{0.3} . \qquad (5)$$

Equating ϑ_I and ϑ_{II}, we are obtaining the criterion for determining the absence of non-stationary nucleate boiling:

$$\left[\frac{2\lambda(\vartheta_0 - \vartheta_I)}{R} \right]^{0.3} \equiv \left[\alpha_{conv} (\vartheta_{II} + \vartheta_{uh}) \right]^{0.3}$$

or

$$Bi = \frac{2(\vartheta_0 - \vartheta_I)}{\vartheta_I + \vartheta_{uh}}, \qquad (6)$$

because in formula (3) $\vartheta_I \equiv \vartheta_{II}$.

Equation (6) is the basic criterion that determines the absence of non-stationary nucleate boiling (self-regulated thermal process) at steel quenching, Ref.(5,6).

3 Intensive Quench Process Interruption to Receive Optimal Hardened Layer

The results of theoretical and experimental investigations for the determination of the heating and cooling time for bodies of various configuration have been generalized by author of [9] and presented in the form of equation (7) convenient for calculations.

Theory of the regular heat conditions describes the process of cooling for bodies of different shapes. The time of cooling of such bodies can be evaluated on the basis of the dimensionless dependence:

$$Fo_v\ Kn = \left[\frac{k\,Bi_v}{2.095 + 3.867\,Bi_v} + \ln\theta\right],$$

$$(7)$$

$$t = \left[\frac{k\,Bi_v}{2.095 + 3.867\,Bi_v} + \ln\frac{T_0 - T_C}{T - T_C}\right]\frac{K}{a\,Kn}.$$

Where t - cooling time; Fo_v - generalized Fourier number; Bi_v -generalized Biot number; k= 1, 2, 3 - correspondingly to bodies of plate, cylindrical and spherical shape; K - Kondratjev form factor; Kn - Kondratjev number; a - thermal diffusivity coefficient; T_0 - initial temperature of heated part; T_C - temperature of the medium; T - current temperature.

According to the patented technology, the process of the intensive cooling should be performed in such a way that the martensite transformations begin uniformly at all the surface simultaneously forming high compressive stresses which, as was noted, achieve the maximum at a definite moment of time. This moment of time can be determined by equation (7). For bodies with different configurations temperatures are found at points the furthest from the surface which correspond to the maximum compressive stresses at the surface. Using this data and formula (7) one can easily calculate time of achieving maximum compressive stresses without making expensive and complicated calculations. The proposed approach is also correct for bodies of complex configurations

4 Quench Process Optimization

The optimal residual stress distribution in the quenched steel part occurs in case of optimal depth of the hardened layer. In this case high compressive stresses at the surface and less tensile stresses in the core are observed. It is fair for any size of a part if the condition (5) is met:

$$\frac{DI}{D_{opt}} = const. \qquad (8)$$

Where DI is the ideal critical diameter or specific size, D_{opt} is size of the steel part with the optimal stress distribution. Ideal critical diameter can be calculated using equation (2).

An optimal residual stress distribution is shown in the Fig. 2. It is of great practical interest to study the effect of the intensity of cooling at quenching on the value of residual stresses which remain in parts after their complete cooling, since the service life of machine parts depends on not only mechanical properties of the material, but also residual stresses. Tensile stresses at the surface of a hardened part reduce its service life, and compressive ones, on the contrary, increase. Besides, tensile stresses result in quench crack formation.

```
9999999999999999999888888888888888888777777777777777777777777776666
 9999999999999999999999999888888888888887777777777777888888777776666
 AAAA9999999999999999999998888888888888888877777778888888887777766 6
 AAAAAAAAAAAA99999999999999998888888888888888888878888888888777776 66
 AAAAAAAAAAAAAAAAAAAAA9999999999999999999888888888888888888877777 66
 AAAAAAAAAAAAAAAAAAAAAAAAAAAAAAAAAAA999999988888888888888888 7777666
 BBBBBBBABBBBBBBBBBAAAAAAAAAAAAAAAAAAAA9999999999999999888887777666
 BBBBBBBBBBBBBBBBBBBBBBBBBBBBAAAAAAAAAAAAA9999999999999998888777666
 BBBBBBBBBBBBBBBBBBBBBBBBBBBBBBBBBBAAAAAAAAA99999999999999888777666
 CCCCCCBBCCCCCCCCCCCCBBBBBBBBBBBBBBBBBAAAAAAAAA99999999999888777666
 CCCCCCCCCCCCCCCCCCCCCCCCCCCCBBBBBBBBBBBAAAAAAAAA999999999988887766
 CCCCCCCCCCCCCCCCCCCCCCCCCCCCCCBBBBBBBBBBAAAAAAAAAAAAAAAA99888777766
 CCCCCCCCCCCCCCCCCCCCCCCCCCCCCCCCBBBBBBBBBBAAAAAAAAAAAAAA999888877776
 CCCCCCCCCCCCCCCCCCCCCCCCCCCCCCCCCBBBBBBBBBBAAAAAAAAAAAAAA999888777777
 CCCCCCCCCCCCCCCCCCCCCCCCCCCCCCCCCCBBBBBBBBBAAAAAAAAABBBAAAA9998877777777777
 CCCCCCCCCCCCCCCCCCCCCCCCCCCCCCCCBBBBBBBBBBBBBBBAABBBBBBAA999888777777777777
 CCCCCCCCCCCCCCCCCCCCCCCCCCCCCBBBBBBBBBBBBBBBBBBBBBBBBBBBAA99988877777777777
 CCBBBBBBBBBCCBBBBBBBBBBBBBBBBBBBBBBBBBBBBBBBBBBBBBBCCCBBBBAA9988887778888888
 BBBBBBBBBBBBBBBBBBBBBBBBBBBBBBBBBBBBBBBBABBBBBBCCCCBBBA99888888888888888888
 BBBBBBBBBBBBBBBBBBBBBBBBBBBBBBBBBBAAAAAAAAAABBCCCDCBBA998888888888888888888
 AAAAAAAABBBBBBBBBBBBBBBBBBBBBBBBAAAAAAAAABBBCCCCCCDB98777777777888888888888
 AAAAAAAAAAAAAAABBBBBBBBBBBBBBBAAAAABBBBBCCDCA877887777777777888888888888888
 AAAAAAAAAAAAAAAAAAAAAAAAAAABBBBBBBBBBCCBBA987777777777888888888888888888888
 EDCCBBBBBBBBBBBBAAAAAAAAAAAABBBBAAAAAAAA99998766667777778888888888888888888
 776AA999999999999988888888888888777777677777777            8888888888888888
 566666666666666666666776666666677777777777777777            8888888888888888
 666677777777777777777777777777777777777778888            8888888888888888
                                                            888888888888888
                                                            8888888888888
```

```
LEGEND

 5 -1000 -  -800
 6  -800 -  -600
 7  -600 -  -400
 8  -400 -  -200
 9  -200 -     0
 A     0 -   200
 B   200 -   400
 C   400 -   600
```

Fig. 2 Hoop residual stress distribution on the cross section of the stamp (steel AISI 52100) after its partial self-tempering and final cooling to room temperature (α=20000 W/m^{2}K)

Table 2 Fatigue tests of KrAZ truck half- axles [1]

Quenching method	Steel grade	Numbers of cycles to fracture	Note
Oil	AISI/SAE 4340	$(3.8 – 4.6)10^5$	Half-axles were destroyed
Intensive water spray cooling	AISI/SAE 1045	$(3.0 - 3.5)10^6$	No fractures observed

Optimum stress distribution on section of steel parts means high compessive stresses at the surface and less tensile stresses at the core. Since cooling rate within the martensite range is very high during intensive quenching, additional strengthening of the material is observed. More detailed information about this phenomenon is discussed in Ref. (3). High compressive stresses at the surface and additional strengthening of material increase significantly the service life of steel parts (see Table 2). Detailed information about optimal stress distribution, service life of truck half-axles and equipment are provided in Ref.(4).

5 Low Hardenability Steels

As is well known, the strength properties of material are high when the grain is finer and the dislocations density are higher too. The high density of dislocations in material can be obtained by the essential increase in the cooling rate within the martensite range. Service life of machine parts can be significantly increased by using low hardenability steels which are intensively quenched. The chemical composition of low hardenability steels are provided in Table 4 and Table 3 [5,6].

Table 3 Chemical composition of some new low-hardenability steels [6]

Element or DI	Chemical composition of steel, wt. %					
	$62PP_1$	$62PP_2$	$62PP_3$	$62PP_4$	62PNP	$80PP_1$
C	0.60-0.67	0.60-0.67	0.60-0.67	0.60-0.67	0.60-0.67	0.78-0.85
Mn	0.05-0.15	$\leq$0.10	0.05-0.15	0.10-0.20	$\leq$0.06	$\leq$0.10
Si	$\leq$0.05	0.10-0.20	0.05-0.15	0.10-0.20	$\leq$0.06	$\leq$0.05
Cr	$\leq$0.10	$\leq$0.10	$\leq$0.10	$\leq$0.10	$\leq$0.06	$\leq$0.10
Ni	$\leq$0.10	$\leq$0.10	$\leq$0.10	$\leq$0.10	$\leq$0.06	$\leq$0.10
Cu	$\leq$0.10	$\leq$0.10	$\leq$0.10	$\leq$0.10	$\leq$0.06	$\leq$0.10
Al	0.03-0.10	0.03-0.10	0.03-0.10	0.03-0.10	0.03-0.10	0.03-0.10
Ti	0.06-0.12	0.06-0.12	0.06-0.12	0.06-0.12	0.06-0.12	0.06-0.12

V	≤0.4	≤0.4	≤0.4	≤0.4	0.2-0.3	≤0.04
S	≤0.04	≤0.04	≤0.04	≤0.04	≤0.04	≤0.04
P	≤0.035	≤0.035	≤0.035	≤0.035	≤0.035	≤0.035
Critical diameter, DI, mm	8-13	8-12	8-13	11.5-15.5	8.5-9.5	10-12

Table 4 Commercial and industrially tested technologies with use of low hardenability steels and intensive quenching [7]

Parts	Steel used for IQ process	Steels and technologies which were replaced
Cylindrical and conical gears of trucks and tractors	58(55PP)	30KhGT and other carburizing steels, carburizing of 10 h.
Cylindrical gears of electric driven train transmissions and locomotives (m=10 mm)	ShKh4	20KhN3A, 20Kh2N4A, carburizing of 30 h.
Small modulated gears (m=4-6 mm) with splined openings (solar, satellite ones)	58(55PP)	18KhGT and others, carburizing of 15 h

Thus, the formation of high-strength materials and increase in the service life of parts quenched is a real prospect if we strictly fulfill three main conditions:

- At first, obtaining the austenite grain as fine as possible (11-14 points);
- Providing the optimal depth of the hardened layer;
- Maintaining the maximal cooling rate during all the process of steel quenching.

Thus, the practice proves that intensive quenching of low-hardenability steels with very fine grain and optimal depth of hardened layer providing high compressive stresses at the surface allows to considerably increase the surface life of parts of machines and equipment of any kind [8–10]. Metallurgists started to design low-hardenability steels [11] for specific parts, which provide the optimal depth of hardened layer and, thus, result in maximal compressive stresses at the surface and not big tensile stresses in the core of the part [12]. The ratio of the depth of hardened surface layer to thickness of the part is 0.2-0.5, which depends on the shape of the part [12-17].

Table 5 Optimal depth of hardened layer with respect to sizes and steel grade of a part to be quenched

Part description and sizes	Steel grade	DI, mm	DI/D_{opt}	DI/D used in practice
Springs of railroad cars of 19-45 mm diameter	55PP	14.8	0.25-0.5	0.33-0.78
Rollers of frictionless bearings of 30-50 mm diameter	ShKh4	30	0.25-0.50	0.6-1
Washing balls of 60-80 mm diameter	70PP	20	0.20-0.30	0.25-0.33
Turbine rotor of 1855 mm in diameter	26Cr2Ni4MoV	417	0.25-0.5	0.23

Due to the application of intensive quenching technology the mechanical properties of the core are improved significantly, high compressive stresses at the working surface of the steel parts occur, very uniform and high hardness of the surface are achieved, meeting the standard requirements.

The mechanical properties of the specimen's core (a cylindrical sample made of 35KhM steel, 70 mm diameter) are given below (seeTable 6).

Table 6 Comparison of mechanical properties in the core of a part of ∅70 mm, made of 35KhM steel, after quenching in oil and aqueous solution of $CaCl_2$ of optimal concentration

Quenchant	Heating, °C	Tempering, °C	Strength, Mpa		A, %	Z, %	a_k, J/cm^2
			R_m	$R_{po.2}$			
Oil	850	540-550	960	775	14	53	54
Aqueous solution	850	550	970	820	17	63	150

As the Table 6 shows, impact strength of the part's core has increased by almost 3 times after intensive quenching. The authors of Ref.(16) have achieved similar results.

6 Optimization of the Chamical Composition of Steel

The Jominy hardness curves can be used to estimate the ideal critical diameter of an alloy. The ideal critical diameter (DI) is the largest bar diameter that can be quenched to produce 50% martensite at its center after being given an "infinite" or "ideal" quench. The ideal quench is one that lowers the surface temperature of an austenitized steel to the bath temperature instantaneously. Under these conditions, the cooling rate at the bar center depends only on the thermal diffusivity of the steel. The ideal critical diameter can be estimated from a Jominy equations:

$$DI = DI_{base} f_{Mn} \cdot f_{Si} \cdot f_{Cr} \cdot f_{Mo} \cdot f_{V} \cdot f_{Cu} \text{ (in)}, \quad (9)$$

$$DI = 25.4\ DI_{base} f_{Mn} \cdot f_{Si} \cdot f_{Cr} \cdot f_{Mo} \cdot f_{V} \cdot f_{Cu} \text{ (mm)}, \quad (10)$$

where f_x is the multiplicative factor for the particular alloying element. The base DI and one set of alloy factors are presented in Table 7. The alloy factors were developed based on data from medium-carbon steels of medium hardenability. These factors and others for steels of particular composition ranges have been incorporated into calculators for quickly making calculations and plots of Jominy end-quench data .The procedure for calculating the hardenability of a steel from the composition includes the following steps:

- Determine the ASTM grain size.
- Determine the chemical composition.
- Determine base DI from carbon content and grain size.
- Determine alloy factors (see Table 7)
- Multiply the factors according to Eq.(9) or (10) to calculate the ideal diameter.

Table 7 Hardenability f_x factors for carbon grain size and selected alloying elements [18]

Percent	Carbon grain size No			The f_x for alloying elements				
	No. 6	No.7	No.8	Mn	Si	Ni	Cr	Mo
0.05	0.0814	0.0750	0.0697	1.167	1.035	1.018	1.1080	1.15
0.10	0.1153	0.1065	0.0995	1.333	1.070	1.036	1.2160	1.30
0.15	0.1413	0.1315	0.1212	1.500	1.105	1.055	1.3240	1.45
0.20	0.1623	0.1509	0.1400	1.667	1.140	1.073	1.4320	1.60
0.25	0.1820	0.1678	0.1560	1.833	1.175	1.091	1.54	1.75
0.30	0.1991	0.1849	0.1700	2.000	1.210	1.109	1.6480	1.90
0.35	0.2154	0.2000	0.1842	2.167	1.245	1.128	1.7560	2.05
0.40	0.2300	0.2130	0.1976	2.333	1.280	1.146	1.8640	2.20
0.45	0.2440	0.2259	0.2090	2.500	1.315	1.164	1.9720	2.35
0.50	0.2580	0.2380	0.2200	2.667	1.350	1.182	2.0800	2.50
0.55	0.273	0.251	0.231	2.833	1.385	1.201	2.1880	2.65
0.60	0.284	0.262	0.241	3.000	1.420	1.219	2.2960	2.80
0.65	0.295	0.273	0.251	3.167	1.455	1.237	2.4040	2.95
0.70	0.306	0.283	0.260	3.333	1.490	1.255	2.5120	3.10
0.75	0.316	0.293	0.270	3.500	1.525	1.273	2.62	3.25
0.80	0.326	0.303	0.278	3.667	1.560	1.291	2.7280	3.40
0.85	0.336	0.312	0.287	3.833	1.595	1.309	2.8360	3.55
0.90	0.346	0.321	0.296	4.000	1.630	1.321	2.9440	3.70
0.95	…	…	…	4.167	1.665	1.345	3.0520	…
1.00	…	…	…	4.333	1.700	1.364	3.1600	…

7 Discussion

Experience gained by numerous studies and industrial use of low-hardenability steels for manufacturing small parts has shown that it is possible to use intensive cooling for their effective thermal strengthening. The service life of these parts increases by several times in spite of the fact that the steel is lowly alloyed and inexpensive. Quench cracks are not formed despite intensive cooling in water streams at the speed of 20 m/s, because high compressive stresses occur at the surface, and not very high tensile stresses occur in the core. A question arises whether intensive quenching in water is possible for large-sized parts made of alloyed steels.

Here it has been proved for the first time that such technology can be successfully applied if DI/D_{opt}=idem conditions are kept while quenching small and large-sized parts, i.e., the ratio of ideal critical size of the part to its real size is the same. This way it was proved that large-sized parts have similar residual stress distribution along the cross-section, that is, high compressive stresses occur at the surface and low tensile stresses occur in the core. It is expedient to quench parts when the conditions are $Bi \to \infty$. Examples of using this method have been presented. Whence it follows that large-sized parts made of alloyed steels can be cooled in water in conditions $Bi \to \infty$. At the same time it is necessary to keep to the condition $DI/D_{opt} \approx 0.2 \div 0.5$.

If the chemical composition of steel is such that this ratio is out of this range, then intensive quenching is interrupted at the time when the optimal hardened layer is achieved, using for calculations the generalized equation:

After a great number of experiments and computations, a simplified method of calculations of optimal steel quenching conditions has been developed. Finally, the essence of this method is as follows:

- A steel grade with certain chemical composition is chosen;
- Ideal critical size for this steel is determined;
- DI/D_{opt} ratio is found for a specific steel part, which must be within the range of $0.2 \div 0.5$;
- The part is cooled in $Bi \to \infty$ conditions;
- Intensive cooling is interrupted when the optimal depth of hardened layer is achieved, using the simplified method of calculation;
- The part is tempered at the temperature Ms or higher.

The combination of proposed method with the further refinement data based on computer simulation is the foundation of steel quenching process optimization.

8 Summary

1. The analytical dependence for the calculation of ideal critical diameter DI has been suggested. The advantage of this method lies in the opportunity to calculate ideal critical sizes of parts for a big variety of geometries on the basis of using respective CCT diagrams.
2. It is discussed in detail the optimal depth of hardened layer providing high compressive stresses at the surface layers and not big tensile stresses in the core. Here the smooth distribution of residual stresses at cross section of parts quenched is observed.
3. The paper discusses the similarity in the distribution of residual stresses at the cross section of parts quenched. It has been shown that the ratio of the ideal critical diameter to diameter of the part quenched should, to have the optimal depth of hardened layer, be constant, that is, $DI/D_{opt} = const$. These facts allows to develop new technologies for large-sized parts on the basis of results obtained with small parts.

References:

1) N.I.Kobasko, *Steel Quenching in Liquid Media under Pressure*, Kyiv, Naukova dumka, 1980, 206p
2) B.Liscic, H.M.Tensi, W.Luty (Eds.), *Theory and Technology of Quenching*, Springer-Verlag, Berlin, 1992, 484p
3) N.I.Kobasko, Steel Superstrengthening Phenomenon, *Journal of ASTM, February 2005, Vol. 2, No 2, Paper ID JAI 12824*, Available on line at www.astm.org

4) N.I.Kobasko, B.K.Ushakov, W.S.Morhuniuk, Design of Intensive Steel Quench Processes, In a *"Handbook of Metallurgical Process Design",* G.E.Totten, K.Funatani, Lin Xie (Eds), Marcel Dekker, New York, 2004, pp. 733-764
5) K.Z.Shepelyakovskii, F.V.Bezmenov, New Induction Hardening Technology. *Advanced Materials & Processes,* Vol. 15, October 1998, pp 225-227
6) Russian Patent No. 2158320, Construction Steel of Low Hardenability. Application No. 99125102 dd. Nov. 29, 1999.
7) B.K.Ushakov, K.Z.Shepelyakovskii, V.M.Fedin, et.al., Development of Through Surface Hardening Method for Heavy-Load Products and Machine Parts, *Stal No. 11,* 2001, pp. 64-68
8) Ukrainian Patent No. 4448, Method of High-Alloy Steel Quenching, Application No. 3579858/SU dd. Apr. 14, 1983
9) Ukrainian Patent No. 56189, Method of Steel Quenching, Application No. 99042228 dd. Apr.20, 1999
10) US Patent No 6,364,974 B1 Quenching Apparatus and Method for Hardening Steel Parts, Filed on April 18, 2000
11) Russian Patent No. 2164536, Method of Construction Low-Alloy Steel Production in Open-Hearth Furnaces, Application No. 2000109772, dd. Apr. 21, 2000
12) N.I.Kobasko, B.K.Ushakov, W.S.Morhuniuk, Design of Intensive Steel Quench Processes, In a *"Handbook of Metallurgical Process Design*", G.E.Totten, K.Funatani, Lin Xie (Eds), Marcel Dekker, New York, 2004, pp. 733-764
13) N.I.Kobasko, W.S. Morhuniuk, *Study of Thermal and Stress-Strain State at Heat Treatment of Machine Parts* (in Russian: *Issledovanie teplovogo i napriazhenno-deformirovannogo sostoyaniya pri termicheskoy obrabotke izdeliy mashinostroeniya*), Znanie, Kyiv, 1983, 16 p
14) N.I.Kobasko, Technological Aspects of Quenching (review), *MiTOM,* 1991, No.4, pp. 2-8
15) N.I.Kobasko, Basics of Intensive Quenching, *Adv. Materials & Processes/Heat Treat. Prog.,* Part I, Vol. 148 (No.3), September 1995, pp. 42W-42Y
16) M.A.Aronov, N.I.Kobasko, J.A.Powell, "Practical Application of Intensive Quenching Process for Steel Parts", *Proceeding of The 2000 Heat Treating Conference,* St. Louse, (2000)
17) N.I.Kobasko, Intensive Steel Quenching Methods. In a Handbook: *Theory and Technology of Quenching* (B. Liščić, H.M.Tensi, W.Luty, Eds.), Springer-Verlag, Berlin, 1992, pp. 367-389
18) G.E.Totten, C.E.Bates and N.A.Clinton, *Handbook of Quenchants and Quenching Technology*, ASM International, 1993, 507 p